On the nature of the variability power decay towards soft spectral states in X-ray binaries. Case study in Cyg X-1

Lev Titarchuk[1,2,3] and Nikolai Shaposhnikov[4]

ABSTRACT

A characteristic feature of the Fourier Power Density Spectrum (PDS) observed from black hole X-ray binaries in low/hard and intermediate spectral states is a broad band-limited noise, characterized by a constant below some frequency (a "break" frequency) and a power law above this frequency. It has been shown that the variability of this type can be produced by the inward diffusion of the local driving perturbations in a bounded configuration (accretion disk or corona). In the framework of this model, the perturbation diffusion time t_0 is related to the phenomenological break frequency, while the PDS power-law slope above the "break" is determined by the viscosity distribution over the configuration. The perturbation diffusion scenario explains the decay of the power of X-ray variability observed in a number of compact sources (containing black hole and neutron star) during an evolution of theses sources from low/hard to high/soft states. We compare the model predictions with the subset of data from Cyg X-1 collected by the Rossi X-ray Time Explorer (RXTE). Our extensive analysis of the Cyg X-1 PDSs demonstrates that the observed integrated power P_x decreases approximately as a square root of the characteristic frequency of the driving oscillations ν_{dr}. The RXTE observations of Cyg X-1 allow us to infer P_{dr} and t_0 as a function of ν_{dr}. Using the inferred dependences of the integrated power of the driving oscillations P_{dr} and t_0 on ν_{dr} we demonstrate that the power predicted by the model also decays as $P_{x,diff} \propto \nu_{dr}^{-0.5}$ that is similar to the observed P_x behavior. We also apply the basic parameters of observed PDSs, power-law index and low frequency quasiperiodic oscillations, to infer Reynolds (Re) number from the observations using the method developed in our previous paper. Our analysis

[1]George Mason University/Center for Earth Observing and Space Research, Fairfax, VA 22030; and US Naval Research Laboratory, Code 7655, Washington, DC 20375-5352; ltitarchuk@ssd5.nrl.navy.mil

[2]Dipartimento di Fisica, Universitá di Ferrara, via Saragat 1, I–44100, Ferrara, Italy; titarchuk@fe.infn.it

[3]Goddard Space Flight Center, NASA, code 661, Greenbelt MD 20771; lev@milkyway.gsfc.nasa.gov

[4]Goddard Space Flight Center, NASA/Universities Space Research Association, code 662, Greenbelt MD 20771; nikolai@milkyway.gsfc.nasa.gov

shows that Re−number increases from values about 10 in low/hard state to that about 70 during the high/soft state.

Subject headings: accretion, accretion disks—black hole physics—stars:individual (Cyg X-1) :radiation mechanisms: nonthermal—physical data and processes

1. Introduction

The main goal of the presented work is to explain a decay of the emergent time variability of X-ray emission in compact sources when these sources evolve from low/hard (LH) to high/soft (HS) states [see Remillard & McClintock (2006) and Titarchuk, Shaposhnikov & Arefiev (2007), hereafter TSA07, for details of observations]. In particular, power density spectrum (PDS) of black hole binaries in hard states is dominated by a component, which has a specific shape roughly described by a broken power-law. The low-frequency part is mostly flat, while the power-law index α above the "break" frequency ν_{br} is variable between 1 and 2. It is well established that the fractional root-mean-square (rms) variability in a source lightcurve decrease as a source evolves from LH state to HS state. Simultaneously, both ν_{br} and α increase. Although empirical shot-noise models were able to describe in general the observed PDS shape (Focke et al. 2005), the physical picture explaining the observed evolution during spectral transitions was missing. Moreover, shot-noise models were challenged by the linear absolute rms-flux relation (Uttley, McHardy & Vaughan 2005; Uttley 2004). This rms flux relation assumes that amplitudes and time-scales of shots are not independent, but are related in some way.

Lyubarskii (1997) was the first to suggest a model for this time variability production in the accretion powered X-ray sources. He considered small amplitude local fluctuations in the accretion rate at each radius, caused by small amplitude variations in the viscosity, and then studied the effect of these fluctuations on the accretion rate at the inner disc edge. His linear calculations show that if the characteristic time-scale of the viscosity variations is everywhere comparable to the viscous (inflow) time-scale, and if the amplitude of the variations is independent of radius, then the power spectrum of luminosity fluctuations is a power-law $1/\nu$. If the amplitude of the variations increases with radius, the slope of the power spectrum of the luminosity variations is steeper than 1. Lyubarskii pointed out that he had no physical model for the cause of such fluctuations. Uttley, McHardy & Vaughan (2005) pointed out that rms-flux relation is naturally explained in the framework developed by Lyubarskii.

TSA07 formulated and solved the problem of local driving perturbation diffusion in a

disk-like configuration. The problem of the diffusive propagation of the space distributed high-frequency perturbations is formulated as a problem in terms of the diffusion equation for the surface density perturbations. This equation is combined with the appropriate boundary conditions. The formulation of this problem and its solution are general and classical. The parameters of the resulting PDS, diffusion time scale of the diffusion propagation of the local perturbations t_0 and the power-law index of the viscosity distribution over the disk-like configuration α, are essential parameters of diffusion in a given bounded configuration. In TSA07 we call our model for the PDS of Green's function of the bounded configuration as a white-red noise (WRN) and we adopt this name throughout this paper.

The problem formulation was similar to the Lyubarskii's scheme. However, the method of solution is different. Lyubarskii treated the factorization of the driving term (i.e. separating it into two parts each depending on time and radius only) by linearizing the system. In TSA07 the analytical solution is obtained for the case of the factorized driving sources. Then, using the mean value theorem we showed that the general solution is simply a convolution of the response (Green's function) signal of the configuration and the mean driving signal in the configuration. Thus the resulting power spectrum of the X-ray signal, as a convolution, is a product of the power spectrum related to the disk-like configuration response (the Green's function) and that related to the perturbation sources (sources of driving oscillations). The Green's function PDS is a white-red noise power spectrum (WRN). Specifically, the low frequency (LF) asymptotic form of the WRN PDS, when the frequency is less than the inverse of diffusion timescale in the disk t_0^{-1}, is characterized by a flat shoulder (white noise). In other words, the LF white noise shoulder is insensitive to the source distribution and to the viscosity law in the disk as a function of radius. The high frequency (HF) asymptotic form of WRN is a power law $\nu^{-\alpha}$ with index α, which is determined by the viscosity and perturbation source distribution over the disk. When the viscosity *linearly* increases with radius and the perturbation sources distribution is quasi-uniform, the index is $\alpha = 3/2$. The basis of the presented power spectrum formation scenario is that the timing signal of the WRN PDS shape is a result of diffusive propagation of driving perturbations in the bounded configuration (disk or Compton cloud) in the same way as X-ray photon spectrum is a result of the photon diffusion (namely, upscattering of seed photons) in the same bounded configuration.

The driving oscillation amplitude is assumed to be a smooth function of the radius. TSA07 suggested that driving fluctuations in the configuration can be introduced by g-mode driving oscillations at any given disk annulus. The local g-mode driving fluctuations, produced possibly by local Rayleigh-Taylor local instabilities are high-frequency damped quasi-periodic oscillations (QPOs) which frequencies are related to the local Keplerian frequencies. As we mentioned above TSA07 formulated and solved a problem of the diffusive propagation

of the space distributed high-frequency perturbations in the bounded configuration.

Our diffusion model for PDS is a product of WRN PDS and the driving source PDS (Lorentzian).

The WRN PDS is a power spectrum of the solution of the initial value (Cauchy) problem which is a linear superposition of exponential shots [see Wood et al. (2001)]. For example, if the driving perturbations are distributed according to the first eigen-function of the diffusion operator then the bounded medium works as a filter producing just one exponential shot as a result of the diffusive propagation of eigen-function distribution of the seed perturbations. In the general case the resulting signal is a linear superposition of exponential shots which are *related* to the appropriate eigen-functions. Furthermore, TSA07 demonstrate that *the observed rms-flux relations* [e.g. Uttley, McHardy & Vaughan (2005)] is naturally explained by our diffusion model. In the framework of the linear diffusion theory the emergent perturbations are always linearly related to the driving source perturbations through a convolution of the disk-response (Green's) function and source distribution.

An important question is what our diffusion model predicts for relative contributions of the WRN PDS and the driving oscillation PDS in the resulting PDS and for a dependence of the integrated PDS power on the driving oscillation frequency. The next question is how this model dependence of the integrated power vs the driving oscillation frequency is related to the observed dependence of that. The answers to these questions are the points of the presented study.

In §2 we refer to details of Cyg X-1 observations with RXTE. In §3 we outline the main features of the diffusion model and related formulas. In §4 we show how the model integrated power vs the driving oscillation frequency fits X-ray data from Cyg X-1. In §5 we present the inferred correlation of Reynolds number with the driving oscillation frequency and the spectral state (photon index). Application of the paper results to the observed index-QPO frequency correlations is discussed in §6. Conclusions follow in §7.

2. Observations

For our analysis we used Cyg X-1 data from the Proportional Counter Array (PCA) and All-Sky Monitor (ASM) onboard *RXTE* [Swank (1999)]. The data are available through the GSFC public archive [1]. In this Paper we present the analysis of a representative subset of *RXTE* observations of Cyg X-1. A reader can find the details of data reduction and analysis

[1] http://heasarc.gsfc.nasa.gov

in Shaposhnikov & Titarchuk (2006) and TSA07. We chose approximately 200 observations to cover the complete dynamical range of the source evolution from low/hard to high/soft state. For the presented analysis we refit PDSs with our new model and we used the results of our previous spectral analysis for photon index Γ.

To fit a PDS we used a sum of our perturbation diffusion model and one or two Lorentzians to account for the Low Frequency Quasi-Periodic Oscillations (LFQPOs). For higher photon inicies, when the source is close to high/soft state, the contribution of the accretion disk variability component sometimes becomes significant. It is observed as an additional power law at the lower frequencies (see TSA07 for details). We fit this component with simple power law, when it is needed.

3. The main features of the model

The resulting variability of X-ray signal is determined by the fluctuations of the luminosity $\Delta L_x(t)$. We assume that the mass accretion rate variations $\Delta\dot{M}(0,t)$ is converted with efficiency ε_{eff} into the variations of the X-ray luminosity, i.e. $\Delta L_x(t) = \varepsilon_{eff}\Delta\dot{M}(0,t)$. TSA07 show that the fluctuations of the resulting X-ray oscillation signal $\Delta L_x(t)$ due to the diffusion of the driving perturbations is

$$\Delta L_x(t) = \int_0^t \varphi(t')Y(t-t')dt', \tag{1}$$

i.e. a convolution of the response (the Green's function) of the disk-like configuration $Y(t)$ (WRN) and the source variability function $\varphi(t)$. The resulting power spectrum is

$$||F_x(\omega)||^2 = ||F_\varphi(\omega)||^2||F_Y(\omega)||^2 \tag{2}$$

where $F_x(\omega)$, $F_\varphi(\omega)$, $F_Y(\omega)$ are Fourier transforms of $\Delta L_x(t)$, $\varphi(t)$, $Y(t)$ respectively. Using the total power of the driving oscillations P_{dr} one can present the driving oscillation PDS as (see Eqs. 22 and B5 in TSA07)

$$||F_\varphi(\nu)||^2_\nu = \frac{\hat{\Gamma}_{dr}P_{dr}/(a\pi)}{(\nu-\nu_{dr})^2 + (\hat{\Gamma}_{dr}/2)^2} \tag{3}$$

where ν_{dr} is the driving oscillation frequency, $\hat{\Gamma}_{dr}$ is a full width of half maximum (FWHM) of the Lorentzian and a constant a varies in the range between 1 and 2 depending on the ratio of $2\nu_{dr}/\hat{\Gamma}_{dr}$:

$$a = 1 + \frac{2\arctan(2\nu_{dr}/\hat{\Gamma}_{dr})}{\pi}. \tag{4}$$

For example $a = 1$ and $a = 2$ when $2\nu_{dr}/\hat{\Gamma}_{dr} \ll 1$ and $2\nu_{dr}/\hat{\Gamma}_{dr} \gg 1$ respectively.

In Fig. 1 we show a typical example of the model fit to the data using Eq. (2). The parameters of PDS continuum for white-red noise component (WRN) $||F_Y(\omega)||^2$ (see for details TSA07) are the diffusion time scale t_0, index of the power-law viscosity distribution ψ and for the driving oscillation component $||F_\varphi(\omega)||^2$ they are ν_{dr} and $\hat{\Gamma}_{dr}$ (see Eq. 3).

The power-law index of the viscosity distribution ψ is related to the power-law index of the red noise in the WRN PDS (see TSA07):

$$\alpha = \frac{3}{2} - \delta = \frac{16 - 5\psi}{2(4 - \psi)} \quad \text{for} \quad \psi > 0$$

and

$$\alpha = 2 \quad \text{for} \quad \psi < 0. \tag{5}$$

The model predicted integrated power is (see TSA07)

$$P_{x,diff} \sim \frac{P_{dr}}{2\pi\nu_{dr}t_0(\mathcal{Q} + 1/4\mathcal{Q})DC} \tag{6}$$

where $\mathcal{Q} = \hat{\Gamma}_{dr}/\nu_{dr}$ is a quality factor for the driving signal and D is a factor of order of unity. Equation (6) was derived use the mean value theorem for the integral of the product of two functions. In TSA07 we assumed that a constant C related to the mean value of $||F_\varphi(\nu)||^2_\nu$ over the frequency integration range is about a few (see Appendix B2 in TSA07 for details). Here we specify and obtain $C-$constant when we compare the model dependence $P_{x,diff}$ on ν_{dr} with the observable P_x on ν_{dr}. In order to make this comparison one should determine the best-fit parameter t_0 and P_{dr} as functions of ν_{dr}. Note that to derive Eq. (6) we also use the fact that the WRN PDS $||F_Y(\omega)||^2$ is normalized to $1/(Dt_0)$ where $D \gtrsim 1$. (see Eq. B16 in TSA07).

Now we follow the method suggested in TSA07 to infer P_{dr} vs ν_{dr} from the observations. Namely, given the fact that the driving PDS is a constant at frequencies $\nu \ll \nu_{dr}$ we have

$$||F_\varphi(\nu)||^2_\nu = ||F_\varphi(0)||^2_\nu = \frac{\hat{\Gamma}_{dr}P_{dr}/(a\pi)}{\nu^2_{dr} + (\hat{\Gamma}_{dr}/2)^2}. \tag{7}$$

Because for any power spectrum $||F(\omega)||^2$

$$||F(\omega)||^2 d\omega = ||F(2\pi\nu)||^2 2\pi d\nu = ||F(\nu)||^2_\nu d\nu$$

we obtain that (compare with Eq. 2)

$$||F_x(\nu)||^2_\nu = (2\pi)^{-1}||F_\varphi(\nu)||^2_\nu ||F_Y(\nu)||^2_\nu. \tag{8}$$

Thus a combination of Eqs. (7) and (8) leads us to determination of the integrated power of the driving oscillations

$$P_{dr} = \frac{a\pi(\nu_{dr}^2 + (\hat{\Gamma}_{dr}/2)^2)}{\hat{\Gamma}_{dr}} ||F_\varphi(0)||_\nu^2 = 2\pi^2 a \frac{\nu_{dr}^2 + (\hat{\Gamma}_{dr}/2)^2}{\hat{\Gamma}_{dr}} \frac{||F_x(0)||^2}{||F_Y(0))||^2}. \quad (9)$$

We remind a reader that the values of ν_{dr} and $\hat{\Gamma}_{dr}$ are the best-fit PDS parameters, $||F_x(0)||^2$ is the observed PDS value at $\nu = 0$ and $||F_Y(0))||^2$ is a value of the normalized WRN PDS at $\nu = 0$. As we mention above the integral of the normalized WRN PDS $||F_Y(\nu))||^2$ over ν is $1/(Dt_0)$.

4. The integrated power vs driving oscillation frequency and photon index

In Figure 2 we present the observed correlation of low frequency QPO centroid ν_L with the driving QPO frequency ν_{dr} (upper panel) and photon index Γ with ν_{dr} (lower panel). These correlations imply that ν_L along with ν_{dr} increase when the source becomes softer. In other words, the emission area [Compton cloud (CC)] contracts when the source evolves to the soft states.

In Figure 3 we also see this effect of CC contraction as anticorrelation of the CC diffusion time scale t_0 with ν_{dr}. The inferred dependence of t_0 vs ν_{dr} can be fitted by the power law $t_0 \propto \nu_{dr}^{-2.13\pm0.14}$.

We infer the integrated power of the driving oscillations P_{dr} vs ν_{dr} (see Eq. 9) and then we obtain the model integrated power $P_{x,diff}$ vs ν_{dr} (see Eq. 6). In Figure 4 we show that the dependence of P_{dr} vs ν_{dr} can be fitted by power law $P_{dr} \propto \nu_{dr}^{-1.8\pm0.16}$. Namely the driving oscillation power P_{dr} decreases when the source (Cyg X-1) goes to softer states. Presumably the decay of P_{dr} with ν_{dr} is also related to the contraction of Compton cloud. The driving oscillations can result from the Rayleigh-Taylor (RT) local instability [see e.g. Chandrasekhar (1961) and Titarchuk (2003)]]. The decay of P_{dr} can be considered as a cumulative effect of the local Rayleigh-Taylor (RT) instability when the effective area of a given configuration (CC) undergoing RT oscillations contracts.

In Figure 5 we present a comparison of the observable PDS integrated power P_x (black filled circle) with the model predicted $P_{x,diff}$ (crosses) (see Eq. 6). One can see that the dependence $P_{x,diff}$ on ν_{dr} is similar to the observable correlation P_x vs ν_{dr}.

Note that we obtain the factor $C \sim 4$ (see Eq. 6) by shifting a set of the values of $P_{x,diff}$ along Y-axis to fall on top of P_x values. The power-law $P_x \propto \nu_{dr}^{-0.48\pm0.03}$ fits the dependence of the theoretical and observable integrated powers vs the driving oscillation frequency.

5. Reynolds number of the accretion flow in Compton cloud configuration

Using the best-fit parameters of the PDS we can also infer the evolution of the physical parameters of the source such as Reynolds number of the accretion flow Re, with the change of photon index Γ. In fact, TSA07 relate t_0 with Re and a magneto-acoustic QPO frequency ν_{MA} as

$$t_0 = \frac{4}{3}\frac{4}{(4-\psi)^2}\left[\frac{V_{MA}R_0}{\hat{\nu}(R_0)}\right]\left(\frac{R_0}{V_{MA}}\right) = \frac{4}{3}\frac{4}{(4-\psi)^2}\frac{\mathrm{Re}}{a_{MA}\nu_{MA}}, \tag{10}$$

where a_{MA} is a numerical coefficient. Formula (10) leads to the equation

$$\mathrm{Re} = 2\pi\left(\frac{a_{AM}}{2\pi}\right)\frac{3}{4}\frac{(4-\psi)^2}{4}(\nu_L t_0) \tag{11}$$

that allows us to infer a value of Re using the best-fit model parameters t_0 and the QPO low frequency ν_L which presumably equals to ν_{MA}. Ultimately we can find the evolution of Re with the photon index Γ given that ν_L, t_0 and the viscosity index ψ evolve with Γ (see Figs. 2-3 and 6).

In Figure 7 we present the inferred Reynolds number as a function of the photon index Γ. We use Eq. (11) where we set $a_{AM} = 2\pi$ (see details of this assumption in TSA07) and the observable correlations of ν_L and t_0 with Γ (see Figs. 2 and 3). One can see that Re−number steadily increases from 10 to 70 when the source evolves from low/hard state to high/soft state. In contrast, TSA07 found that Re $\sim 8 \pm 2.5$. We note, however, that in TSA07 only WRN model was used without accounting for driving oscillation distribution, which significantly affects the resulting value for ψ. They also used a limited set of data.

Note the observed behavior of the Re-number vs Γ and mass accretion rate was predicted by Titarchuk, Lapidus & Muslimov (1998), hereafter TLM98, where they formulated a transition layer model (TLM) and studied its consequences for observations. It is important to emphasize that the Re−number along with the photon index Γ, the low frequency QPO ν_L and the driving frequency ν_{dr} can be considered as characteristics of the spectral state. All of them correlate with each other.

6. Photon index-QPO frequency correlation

TLM98 showed that the outer (adjustment) radius of the transition layer R_{out} measured in the dimensionless units with respect to Schwarzschild radius $R_S = 2GM/c^2$, $r_{out} = R_{out}/R_S$, anticorrelates with Re−number or photon index Γ (spectral state) only. Thus ν_L (or ν_{MA}) as a ratio $\sim V_{MA}/R_{out}$ should correlate with Γ (or Re−number) where values ν_L related to the same Γ for different sources should be inversely proportional to a mass of

the central object (black hole or neutron star). Note that a plasma velocity V_{MA} is also a function of Γ only. The comparison of the observed index–QPO frequency correlations for two different sources (with two different masses) should lead to determination of their relative masses with respect each other. This is the main idea behind the method of weighing black holes (TLM98) recently applied for BH mass determination in a number of Galactic and extragalactic sources [see Titarchuk, & Fiorito (2004); Fiorito & Titarchuk (2004); Dewangan, Titarchuk & Griffiths (2006); Strohmayer et al. (2007) and Shaposhnikov & Titarchuk (2007)].

7. Conclusions

We explain the decay of the emergent time variability of X-ray emission in compact sources when these sources evolve from low/hard to high/soft states. We find that the resulting power P_x from Cyg X-1 decays with the driving oscillation frequency ν_{dr} as $P_x \propto \nu_{dr}^{-0.5}$.

We show that the reciprocal of the diffusion time scale of the perturbation t_0^{-1}, the low frequency QPO ν_L, the driving oscillation frequency ν_{dr}, inferred by fitting the Cyg X-1 PDSs with our diffusion model, increase when the source evolves from low/hard state to high/soft state. This behavior of the PDS characteristics implies that the Compton cloud contracts towards softer spectral states. The driving oscillations are probably caused by the local Rayleigh-Taylor instability which cumulative P_{dr} decreases when the effective area of the configuration producing the RT oscillations contracts. The decay in driving power leads to the decay in the total observed variability power from the source. Using the fact that t_0^{-1}, ν_L, ν_{dr} increase with Γ and P_{dr}, P_x decrease with Γ we conclude, as a result of our analysis, that the Compton Corona shrinks when Cyg X-1 goes from low/hard state to high/soft state.

Our extensive data analysis of the power spectra from Cyg X-1 with an application of the method of Re−number determination developed in TSA07 indicates that Re related to Compton cloud configuration increases from values about 10 in low/hard state to that about 70 in high/soft state. We confirm the predictions by TLM98 that Re−number should increase with index and QPO frequencies. Thus one can conclude that the observable index-QPO correlation is probably driven by the increase of Re−number when the source evolves from low/hard state to high/soft state. It is worth noting that inverse proportionality of the low-frequency QPO with respect BH mass in the index-QPO correlation leads to the method weighing BHs employing this index-QPO correlation.

REFERENCES

Chandrasekhar, S. 1961, *Hydrodynamics and Hydromagnetic Stability*, Oxford: Oxford at the Caredon Press

Dewangan, G., Titarchuk, L. & Griffiths, R. 2006, ApJ, 637, L21

Fiorito, R., Titarchuk, L. 2004, ApJ, 614, 2, L113

Focke, W. B., Wai, L. L., & Swank, J. H. 2005, ApJ, 633, 1085

Lyubarskii, Yu., E. 1997, MNRAS, 292, 679 (L97)

Remillard, R. A. & McClintock, J. E. 2006, ARA&A, vol. 44, 49

Shaposhnikov, N. & Titarchuk, L. 2007, ApJ, in press (astro-ph/0602091)

Shaposhnikov, N. & Titarchuk, L. 2006, ApJ, 643, 1098

Strohmayer, T. E., Mushotzky, R. F., Winter, L., Soria, R., Uttley, P., & Cropper, M. 2007, ApJ, 660, 580

Swank, J. H. 1999, Nucl. Phys. B - Proc. Suppl., 69, 12, 569, 362

Titarchuk, L., Shaposhnikov, N. & Arefiev, V. 2007, ApJ, 660, 556 (TSA07)

Titarchuk, L. 2003, ApJ, 591, 354

Titarchuk, L.G. & Fiorito, R. 2004, ApJ, 612, 988 (TF04)

Titarchuk, L., Lapidus, I.I., & Muslimov, A. 1998, ApJ, 499, 315 (TLM98)

Uttley, P., McHardy, I.M., & Vaughan, S. 2005, MNRAS, 359, 345

Uttley, P. 2004, MNRAS, 347, L61

Wood, K. S., Titarchuk, L., Ray, P.S., et al. 2001, ApJ, 563, 246 (W01)

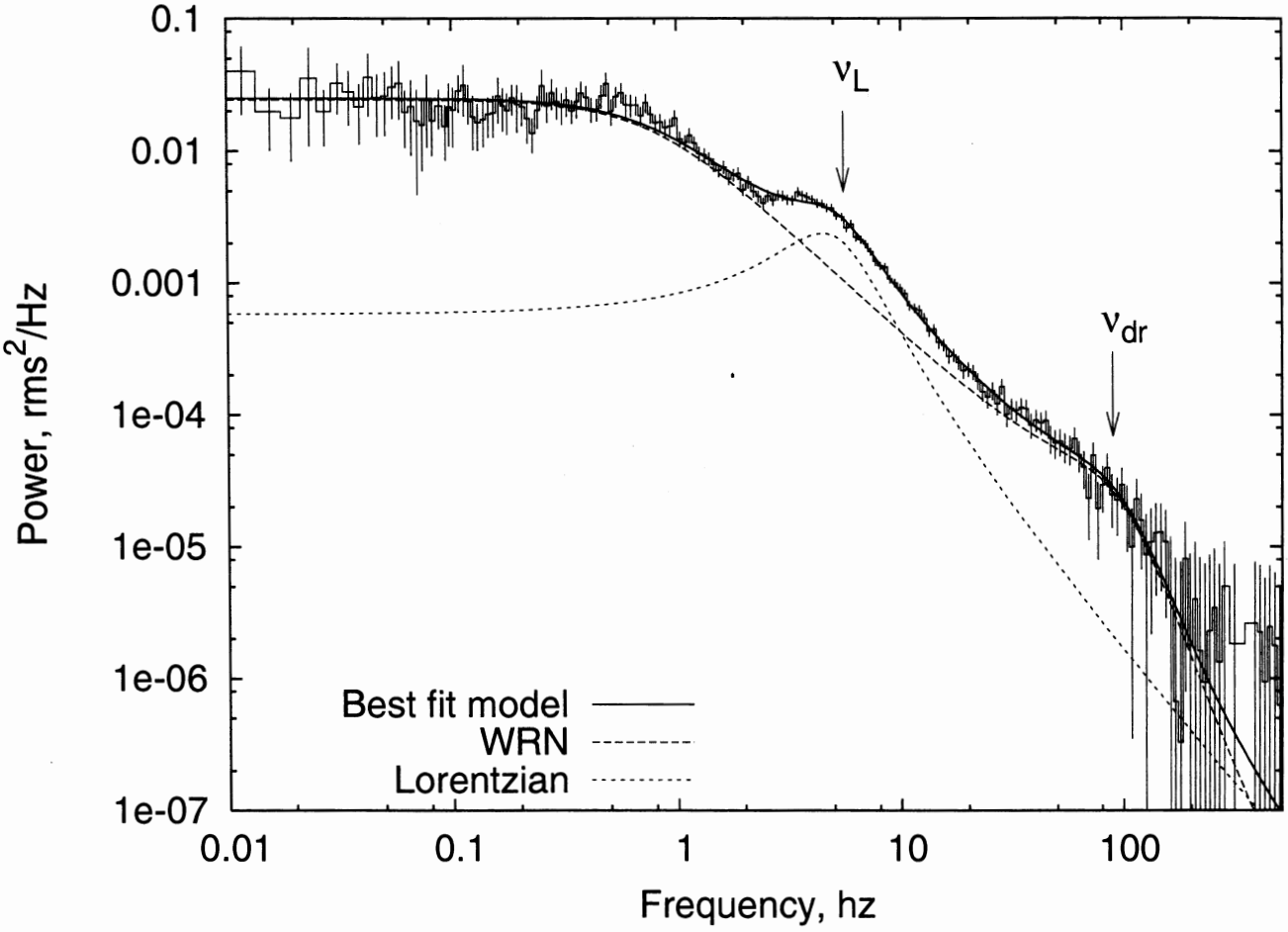

Fig. 1.— A particular example of observable PDS. The PDS continuum is fitted by our diffusion PDS model which is a product of WRN PDS and the driving oscillation Lorentzian. We also use a simple Lorentzian to fit QPO features.

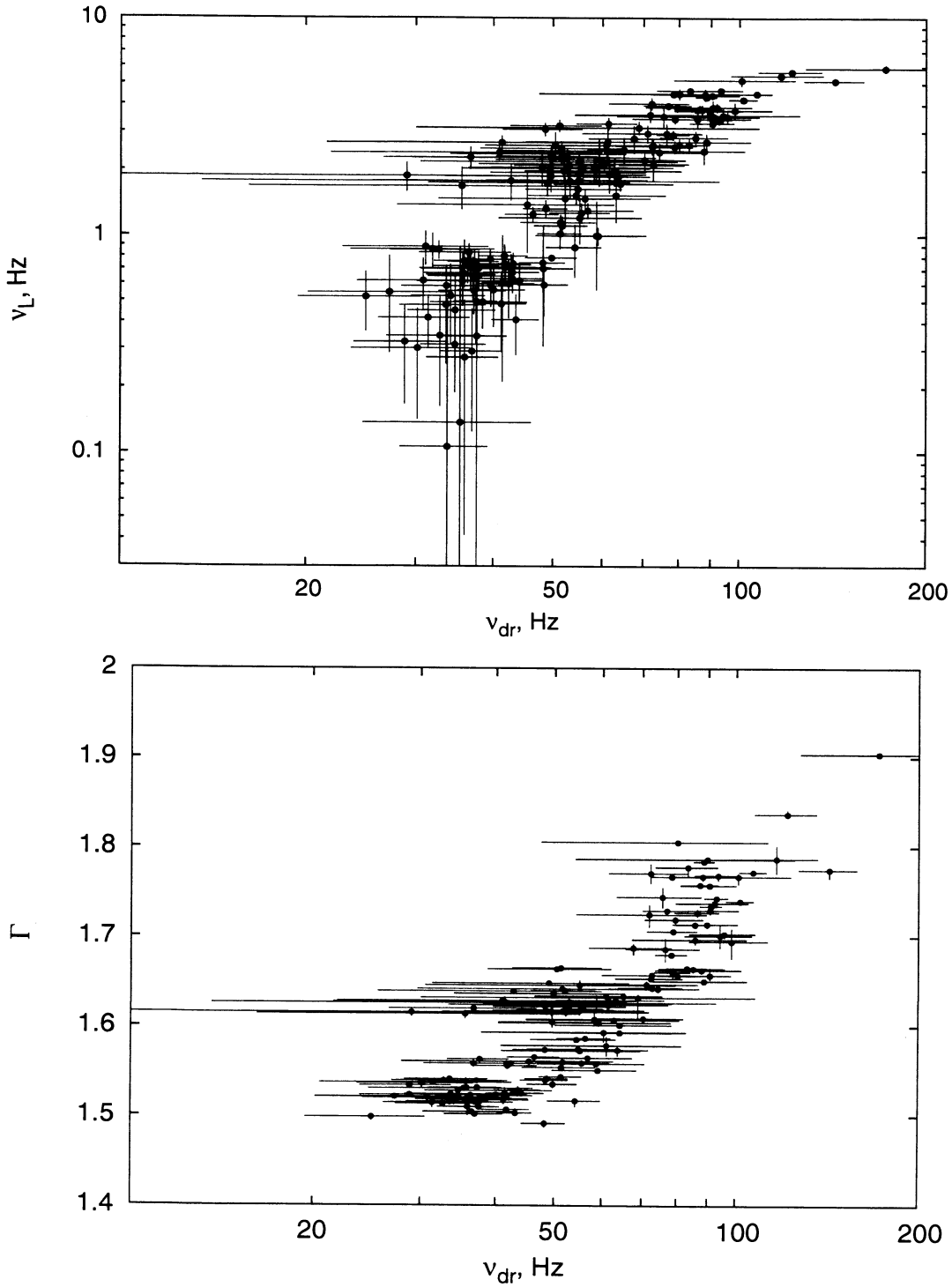

Fig. 2.— Upper panel: low QPO frequency ν_L vs driving QPO frequency ν_{dr} lower panel: photon index Γ vs ν_{dr} .

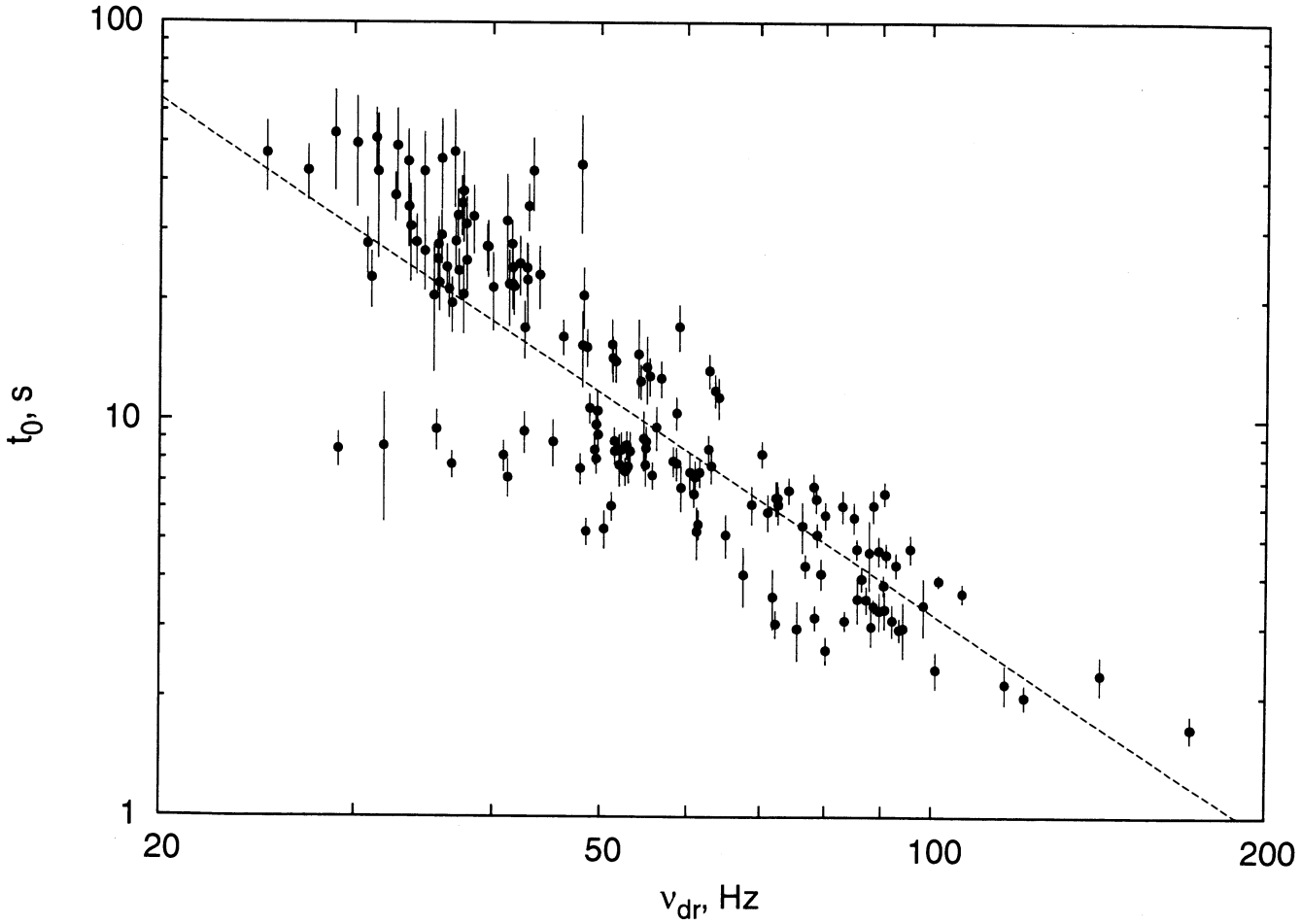

Fig. 3.— The best-fit model parameter, diffusion time scale t_0 vs ν_{dr}. The dashed line is the best fit power law $t_0 \propto \nu_{dr}^{-2.13\pm0.14}$.

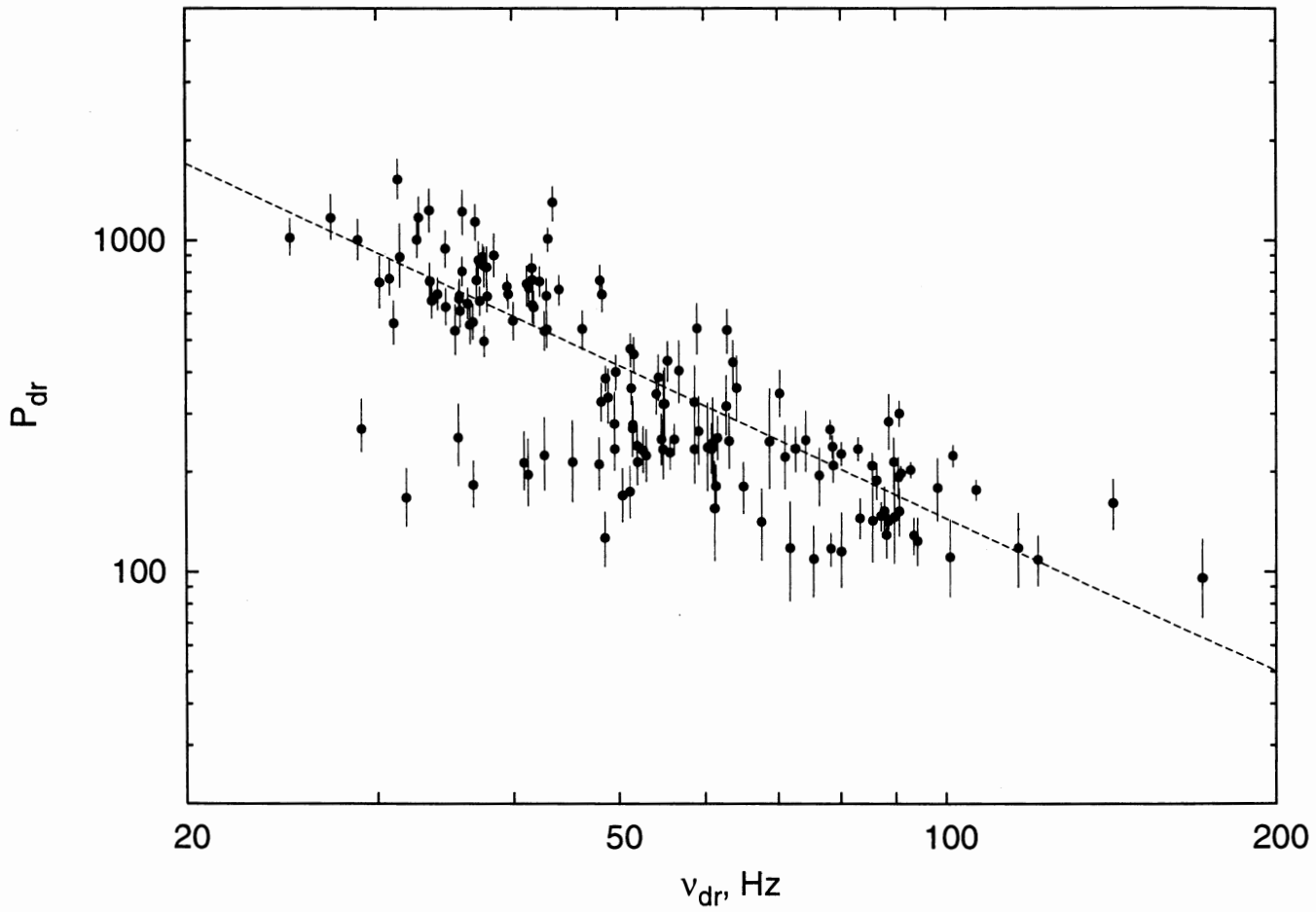

Fig. 4.— Inferred P_{dr} vs ν_{dr}. The dashed line is the best fit power law $P_{dr} \propto \nu_{dr}^{-1.8\pm0.16}$.

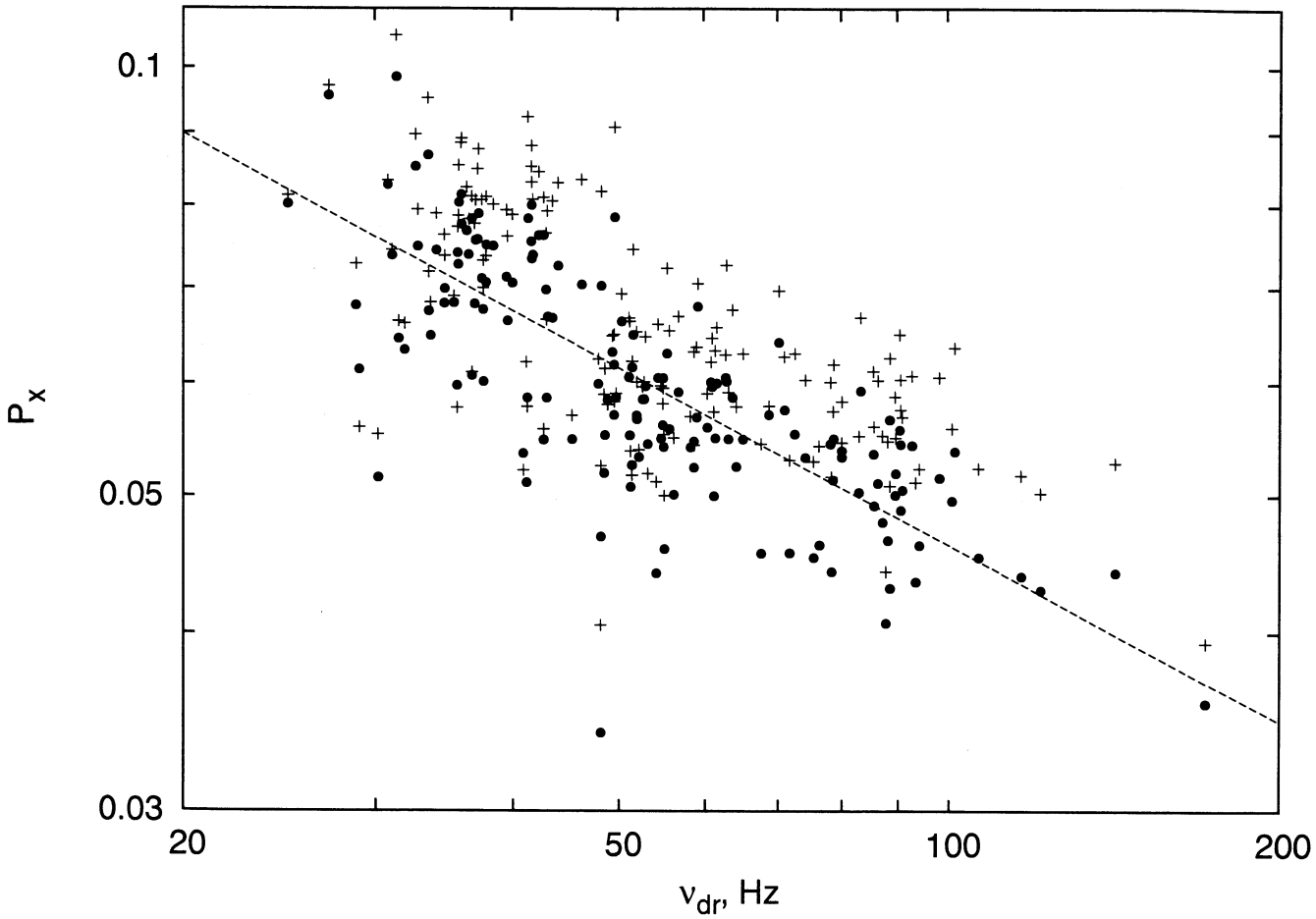

Fig. 5.— Comparison of the model $P_{x,diff}$ vs ν_{dr} (crosses) (using Eq. 6) with the observable P_x vs ν_{dr} (black filled circle) The dashed line is the best fit power law $P_x \propto \nu_{dr}^{-0.48\pm0.03}$.

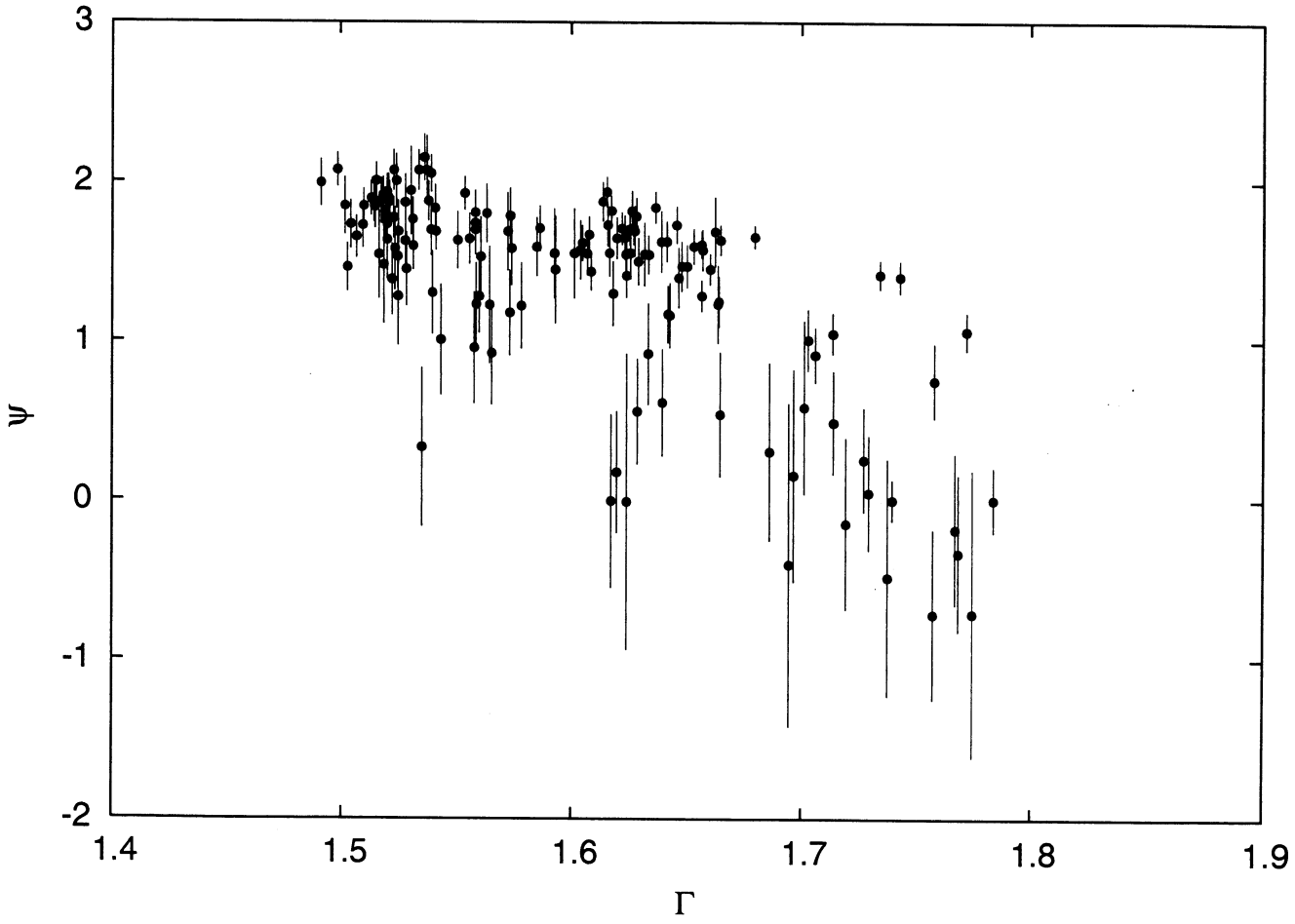

Fig. 6.— The best-fit index of the viscosity distribution ψ vs Γ.

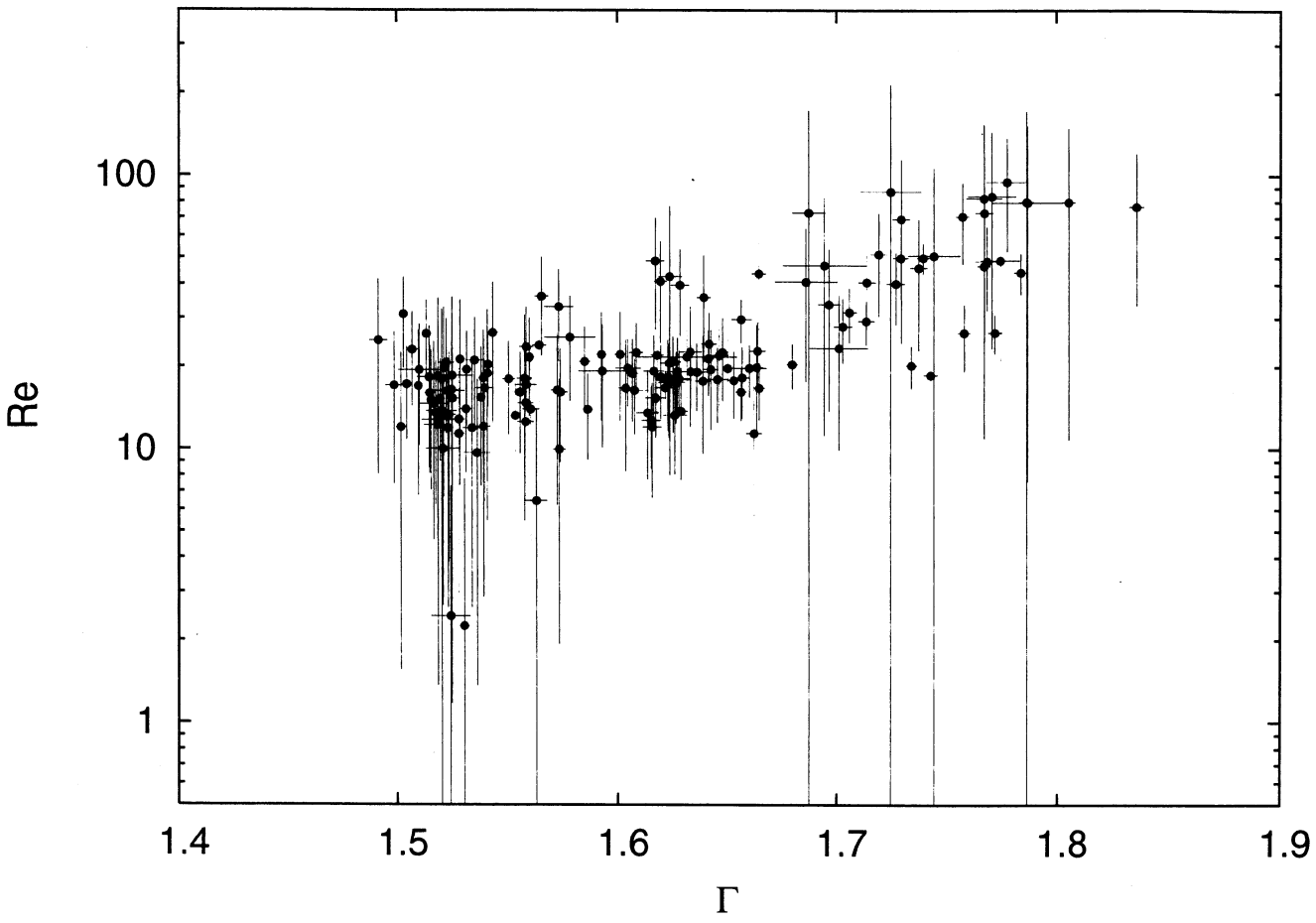

Fig. 7.— Inferred Reynolds number Re (using t_0, ν_L, $\dot{\psi}$, and Eq. 11) vs Γ.